RESEARCH ARTICLE

Human Skin is Permselective for the Small, Monovalent Cations Sodium and Potassium but not for Nickel and Chromium

TERRI D. LA COUNT, GERALD B. KASTING

Winkle College of Pharmacy, The University of Cincinnati Academic Health Center, Cincinnati, Ohio

Received 3 January 2013; revised 31 March 2013; accepted 9 April 2013

Published online in Wiley Online Library (wileyonlinelibrary.com). DOI 10.1002/jps.23579

ABSTRACT: The molar conductance of excised human skin (Λ_{skin}) immersed in electrolyte solutions comprising four cationic (Na^+, K^+, Ni^{2+}, and Cr^{3+}) and five anionic (Cl^-, NO_3^-, SO_4^{2-}, CrO_4^{2-}, and $Cr_2O_7^{2-}$) species was determined as a function of concentration in Franz diffusion cells. Cation transport numbers for four of these electrolytes were measured in Franz cells by the electromotive force method. Parallel experiments were conducted in solutions alone to establish the validity of the technique. Molar conductance decreased with increasing concentration, following the Kohlrausch law, over a 4–12-fold concentration range. Molar conductance and cation transport values at infinite dilution were extrapolated from these data and used to estimate ionic conductances at infinite dilution. These values were subsequently used to calculate limiting ion mobilities and diffusivities in solution and skin. Results for skin showed the expected increase in cation permselectivity for monovalent cations and a 40–110-fold reduction in effective diffusivities with respect to those in solution. However, Ni^{2+} and Cr^{3+} were relatively less mobile in skin than in solution. Salt diffusivities calculated from ionic mobilities in skin provided a partial explanation for the difference in allergenic potency of $NiCl_2$ compared with $NiSO_4$ and Cr^{3+} versus Cr^{6+} salts. © 2013 Wiley Periodicals, Inc. and the American Pharmacists Association J Pharm Sci

Keywords: skin; permeability; mobility; membrane conductance/resistance; iontophoresis; membrane transport; polar pathway; mathematical model; nickel; chromium

INTRODUCTION

The skin has often been stated to be permselective for cations, based on electro-osmotic flow[1] and sodium ion transference numbers.[2–4] But, is this true for all cations or just the ones that dominate electro-osmotic flow? How does this permselectivity impact the absorption of hazardous metal allergens (e.g., Ni^{2+} and Cr^{3+}) or potentially allergenic quaternary ammonium salts (e.g., cationic hair dyes) when they contact the skin either as simple salts or as components of more complex electrolyte solutions? Can characterization of the skin transport properties of a selected set of electrolytes, in combination with appropriate electrodiffusion models, lead to an improved capability to assess the risk associated with dermal exposure to these substances? We hold that the answers to all of these questions are important, a position supported by a recent request for proposals from the European chemical industry for skin absorption models that can (among a list of objectives) effectively deal with the skin permeation of charged and other highly hydrophilic substances.[5]

Considering that there is already a book on metal ion absorption through the skin[6] and that sophisticated models for the skin's polar pathway have been available for a decade,[7–9] one might anticipate that the experimental and theoretical basis for a predictive model of ion permeation through skin has already been established. This, in fact, was our expectation when we set about trying to produce such a model under National Institute of Occupational Safety and Health sponsorship (R01 OH007529). However, a close examination of these sources, described below, convinced us that an unambiguous formulation of the polar pathway, as it applies to passive permeation of charged substances, was not yet possible. This finding was an impetus for the work described here, as well as an additional theoretical development that will be reported elsewhere.

Additional Supporting Information may be found in the online version of this article. Supporting Information

Correspondence to: Gerald B. Kasting (Telephone: +513-558-1817; Fax: +513-558-0978; E-mail: Gerald.Kasting@uc.edu)

Journal of Pharmaceutical Sciences

© 2013 Wiley Periodicals, Inc. and the American Pharmacists Association

The permeation of common metal allergens through skin has been studied using both *in vitro* [10–21] and *in vivo*[6,10,22–24] methodologies; a summary of metal salt absorption data through the 1990s can be found in Ref. 6. However, a close examination of these data reveals a wide variation in experimental conditions and a lack of comparative data obtained under standardized conditions; consequently, a systematic understanding of metal salt absorption has not yet been achieved. Outstanding questions include the following: Can the low permeability of Cr^{3+} be attributed to its binding with epidermal tissue or should it be ascribed to olation and, hence, steric hindrance?[25] Can the observation that nickel chloride is a more potent allergen than nickel sulfate[26] be quantitatively related to skin permeation? For chromium, an apparent dichotomy exists between the actual elicitor of the immunological response (Cr^{3+})[27] and the oxidation state that more readily permeates skin (Cr^{6+}).[17] This, however, can be explained by the small but significant reduction capability of the skin, whereby Cr^{6+} is converted to Cr^{3+}.[27] The risk associated with such exposures is presently addressed on a case-by-case basis with little theoretical guidance. How should one best approach the estimation of electrolyte skin permeation, and what specific factors should be included for a more accurate risk assessment for metal allergen exposures?

Seemingly unrelated literature discusses the polar pathway in skin[7,9,28–32] and the perturbing effect of hydration, electrical fields, and acoustical fields thereon.[9,30,32–36] Sophisticated theories to explain these effects have been proposed, with at least two allowing extrapolation to the passive permeability limit.[30,35] However, the existing theories do not, in our hands, lead immediately to predictions of the passive skin permeation of metal salts or of other potentially hazardous ionic species. A specific objective of our work was to develop a polar pathway theory that yields useful predictions for metal allergen permeation through skin following a consumer or workplace exposure.

The present study represents a step toward this objective. Our aim in this investigation was to determine whether electrical resistance and electromotive force (EMF) measurements of hydrated excised skin immersed in appropriate electrolyte solutions could be used to estimate ion mobilities in the skin's polar pathway. Because the mobilities are intimately related to salt diffusivities under passive conditions,[37,38] a successful application of this approach could lead to rapid characterization of the skin transport parameters for a wide variety of ions. To this end, molar conductance determinations for 10 aqueous electrolytes comprising four cations (Na^+, K^+, Ni^{2+}, and Cr^{3+}) and five anions (Cl^-, NO_3^-, SO_4^{2-}, CrO_4^{2-}, and $Cr_2O_7^{2-}$,) were made as a function of electrolyte concentration. Cation transport numbers for the four chloride salts were determined by an independent method—the EMF method—involving measurement of diffusion potentials. Extrapolation of both the conductances (via the Kohlrausch law[38]) and transport measurements to infinite dilution, followed by subsequent analysis, led to the estimates of ionic conductances and mobilities in skin. Parallel experiments conducted in the absence of skin allowed verification of the test method through comparison of limiting molar conductances and cation transport numbers with literature values. Finally, the ratio of conductance measurements in skin and solution allowed an interpretation of the parameters utilized in the polar pathway theory, yielding the basis for a predictive algorithm.

MATERIALS AND METHODS

Electrolyte Solutions

$K_2Cr_2O_7$, K_2CrO_4, Na_2CrO_4, $Na_2Cr_2O_7$, $Ni(NO_3)_2$, $NiSO_4$, and $CrCl_3$ were purchased from Sigma–Aldrich (St. Louis, Missouri) with a stated purity of greater than 99.5%. NaCl and $NiCl_2$ were purchased from Fischer Scientific (Fair Lawn, New Jersey) with a stated purity of greater than 95%. Conductivity standard KCl solutions were purchased from LabChem Inc. (Pittsburg, Pennsylvania). All electrolytes except KCl were received in solid form and were dissolved in deionized (DI) water obtained from a commercial filtering system (US Filter/Siemens Water, Lowell, Massachusetts, set point 15.62 MΩ cm at 25°C) to prepare stock electrolyte solutions: 0.154 M NaCl and KCl, and 0.0775 M for the remaining solutions. Six to eight serial dilutions were made from each stock solution. The concentrations employed in the analysis were 0.0125−0.154 M for NaCl and KCl, 0.0125−0.0775 M for $NiCl_2$, 0.0206−0.0775 M for $CrCl_3$, and 0.0163−0.0775 M for the remainder of the solutions, respectively. Tests with NaCl and $NiCl_2$ showed that lower concentrations yielded anomalously high molar conductivity values in our apparatus.

Solution Conductivity Measurements

Modified Franz diffusion cells (0.79 cm^2) maintained at 32°C in aluminum blocks were utilized for all experimental procedures.[39] For the solution measurements, the cells were filled with the appropriate electrolyte solution to a level approximately 0.5 cm above the ground glass joint. A four-terminal AC resistance technique was employed, with both driving and sensing electrodes in each compartment. The Ag/AgCl electrodes were constructed from 5 cm lengths of an Ag wire (1.0 mm diameter; ~99.999%; Alfa Aesar, Ward Hill, Massachusetts) electrolyzed in a 0.1 N HCl

solution. These electrodes were placed in a series with an Agilent Model 33220A waveform generator (Agilent Technologies, Santa Clara, California), a 98.28 kΩ resistor (to establish a reference voltage), and a 1 MΩ resistor (to limit current in the circuit). A sinusoidal signal, 20 Hz and 10 Vp-p, was generated by the waveform generator, and the voltage drop across the sensing electrodes was measured with a Keithley Model 175A digital multimeter (Keithley Instruments, Cleveland, Ohio). These settings correlate to a root mean square (RMS) AC current of approximately 7 μA, which is well below that commonly used in iontophoresis. A switch box allowed the procurement of the voltage across the 98.28 kΩ resistor, and the ratio of the voltage drops yielded the solution resistance R_{soln}. Electrolyte solutions were tested in order of increasing concentration to minimize the chance of contamination, with thorough rinsing between solutions of different concentration or composition.

Electrode design and placement were found to be important in obtaining reproducible measurements. To ensure point-source functionality of the electrodes, the entire length of each electrode was encased in a heat-shrink tape, allowing only the tips to remain exposed. The electrodes for each compartment were also taped together to provide extra stability as well as to ensure the maintenance of parallel, equidistant electrode tips. Taping also allowed for uniform electrode orientation during insertion into the ports, and served as an insertion marker for consistency of depth. All of these factors were important for electrical measurement reproducibility.[40]

The cell parameter K, corresponding to the effective ratio of the path length l to cross-sectional area A, for the diffusion cells was obtained by calibration with 0.154 M NaCl. Reproducibility considerations in solution measurements and geometrical restrictions in skin resistance experiments necessitated the use of two different electrode separation distances, and hence, cell parameters. The K values determined from these measurements were 1.47 and 5.06 cm^{-1} for solution and skin experiments, respectively. Solution resistance R_{soln} (Ω) was converted to specific resistivity ρ (Ω cm) according to $\rho = R_{soln}/K$, and specific conductivity σ (Ω^{-1} cm^{-1}) was calculated as $\sigma = 1/\rho$. Molar conductance Λ_{soln} (cm^2 mol^{-1} Ω^{-1}) for each solution concentration was then calculated as $\Lambda_{soln} = \sigma/c$, where c is the electrolyte concentration expressed in mol cm^{-3}.

Skin Conductivity Measurements

Split-thickness human cadaver skin (350–400 μm) from seven donors was obtained from The New York Firefighters Skin Bank (New York, New York). All samples were posterior torso specimens from male donors of varying ethnicity. The skin was kept frozen at −80°C until use. Just prior to use, the skin was quickly thawed by immersion in distilled water, then immediately mounted in the diffusion cells. Both surfaces were hydrated overnight in DI water with the receptor solutions maintained at 37°C, yielding a skin surface temperature of about 32°C. This hydration procedure allowed any mobile endogenous ions to leach out of the tissue. After 24 h, the cells were emptied and five of the six cells were refilled with the lowest concentration of the test solution. The remaining cell was filled with the corresponding concentration of NaCl to serve as a control. Conductivity measurements were carried out as described above, and the process was repeated for the remaining solutions. Skin samples displaying a resistance R_{skin} less than 25 kΩ at any time during the study were rejected, based on literature reports[4,40,41] that specified this as an acceptable criterion for *in vitro* skin integrity. Each electrolyte was tested on three skin donors, with a minimum of five replicates per donor. Overall, 30 experiments were conducted for a total of 180 skin conductivity measurements.

Transport Number Measurements

Solution and skin cation transport numbers were obtained by the EMF method[42] for the four electrolytes containing chloride, as it was necessary to have an ion in common with the Ag/AgCl electrodes to conduct these experiments. Transport number experiments utilized electrolyte concentrations ranging from 0.0125 to 0.154 M (NaCl, KCl) or 0.0125 to 0.0775 M ($NiCl_2$, $CrCl_3$). Two dialysis membranes [previously prepared by soaking first in DI water, then a 30:70 (v/v) EtOH–water mixture, followed by a thorough rinse] were mounted in Franz diffusion cells, with the skin measurements utilizing an additional intervening layer of skin. The rationale for this technique was to reduce any spurious contributions to transport measurements via release of endogenous high-molecular-weight electrolytes from the skin.[42] The system was equilibrated for 24 h. During this time, both compartments were filled with the maximum electrolyte concentration, and the solutions were stirred to minimize the boundary layer effects. Ag/AgCl electrodes were likewise simultaneously conditioned in a separate vial of electrolyte. Prior to each experiment, both compartments were emptied, then refilled with the maximum concentration in the donor compartment and the lowest concentration in the receptor compartment. The equilibrated electrodes were inserted into both the donor and receptor compartments and connected to an Agilent Model 34410A digital multimeter (Agilent Technologies, Santa Clara, California). Voltage measurements were recorded after the values stabilized (10–30 min).

The measurements were repeated for the remaining electrolyte concentrations by exchanging the contents of the receptor compartment only; the donor compartment consistently remained at the maximum concentration. Solution experiments were conducted at ambient (25 ± 2°C) conditions, and skin values were obtained with the receptor solution maintained at 37°C, yielding a skin surface temperature (and donor solution temperature) of 32°C.

Resistance Measurements as a Function of Immersion Time

The resistances of representative skin samples were measured in normal saline over an extended time period to determine the effects of initial hydration and extended immersion. Split-thickness cadaver skin was mounted in diffusion cells ($n = 6$) with the stratum corneum surface open to ambient air and the dermis bathed in 0.154 M NaCl (unbuffered) for a minimum of 4 h. The pH range of these solutions (determined in separate but comparable experiments) was 6.2–6.8 initially and 6.0–6.5 after equilibration with skin, respectively. Saline solution was then introduced into donor compartment and the skin resistance was measured as previously described. Subsequent readings were taken every minute and then at gradually increasing time intervals until 48 h had elapsed. This procedure was repeated for three skin donors. The experiments were then repeated using phosphate-buffered saline with a measured pH of 7.35.

Data Analysis

The conductance data for each diffusion cell were analyzed individually, then averaged over all the cells to obtain a mean value of Λ_{soln} or $\Lambda_{\text{skin+soln}}$ and its standard deviation at each concentration tested. These values were regressed as a function of $\sqrt{c}$ according to the Kohlrausch law (Eq. 1)[38,43,44] to obtain limiting molar conductances at infinite dilution, Λ^0, that is:

$$\Lambda = \Lambda^0 - Ac^{1/2} \tag{1}$$

The limiting molar conductance for skin, Λ^0_{skin}, was calculated from $\Lambda^0_{\text{skin + soln}}$ and Λ^0_{soln} by subtracting the reciprocals (because the resistances $R = 1/\Lambda$ are additive), then inverting the result. The correction for solution resistance was small, averaging less than 7%. Electrolyte theory suggests that Λ^0 can be decomposed into additive contributions from the individual ionic species according to the Kohlrausch law of independent migration:

$$\Lambda^0 = \sum \nu_i \lambda_i \tag{2}$$

where ν_i is the number of ions of species i per mole of salt[45] and λ_i is the limiting equivalent ionic conductance of the species.[38] We made the assumption that such a relationship would hold for both solution and skin. Transport number, $t_\pm$, was obtained from EMF measurements according to the relationship[45]

$$\text{EMF} = \frac{\upsilon}{\upsilon_\pm}\frac{RT}{F}\frac{t_\pm}{z_\pm}\ln\frac{C_2\gamma_{\pm 2}}{C_1\gamma_{\pm 1}} \tag{3}$$

where $\upsilon = \sum \upsilon_\pm$ is the total number of cations and anions per mole of salt; $z_\pm$ is the valence of the ion of interest; C_2 and C_1 are the donor and receptor electrolyte concentrations; γ_2 and γ_1 are the respective activity coefficients; and R, T, and F have their customary meanings of gas constant, absolute temperature, and Faraday's constant, respectively. Transport numbers measured in this manner correspond to the ion that is not reversible with the chosen electrode, and hence in this situation represent t_+.[45] Transport numbers at infinite dilution, $t^0{}_+$, were extrapolated by a linear regression on C_{M}, the average of the donor and receptor concentrations. Cation transport numbers and the corresponding values for anions were also calculated via limiting ionic and molar conductances according to Eq. 4

$$t_i^0 = \nu_i\lambda_i^0/\Lambda^0 \tag{4}$$

The 10 electrolytes studied contained nine distinct ionic species—four cations and five anions. The conductance data thus led to 10 relationships of the form of Eq. 2. The transport number data for the four chloride salts led to four additional, independent relationships of the form of Eq. 4. Reported values of λ_i for both solution and skin were determined by optimizing the values of λ_i in these 14 equations using a nonlinear least-squares procedure (SigmaPlot; SysStat Software, San Jose, California). The weights for the conductance measurements and transport number measurements were chosen as the reciprocal of the average variance $\overline{\sigma^2}$ of the Λ^0 and $t^0{}_+$ determinations, respectively. This procedure, which corresponds to "experimental weighting" as described by Bevington,[46] appropriately adjusts the regression for different magnitudes and uncertainties of the two classes of data. It should be noted that the problem of determining λ_i from the conductance data alone is not well posed, as the equations are linearly dependent.

The uncertainties in the optimized values of λ_i were determined by an auxiliary procedure in which the value of λ_i for each ion was systematically varied around the optimum; the regression for the other eight λ_i was repeated, and the sum of squared residuals (SSR) was recalculated. Confidence limits on the λ_i in question at two levels of uncertainty, 95% and 67%, were calculated by means of an F-test on the

 DOI 10.1002/jps

ratio of SSR to its value at the optimum, SSR_{min}.[46] As there were 14 equations and nine unknowns in these fits, there were five degrees of freedom and the critical values of F were 4.39 (95% confidence) and 1.49 (67% confidence). Thus, the confidence limits reflect the values of λ_I at which SSR was increased by factors of 4.39 and 1.49, respectively.

Conventional (not absolute) mobilities u_i at infinite dilution were calculated according to Eq. 5:

$$u_i = \lambda_i / |z_i| F \tag{5}$$

where λ_i is expressed on a molar basis, and z_i is the valence. Conventional mobilities are generally used in electrochemistry, as they represent the drift velocities under the force exerted by a unit electric field (1 V cm^{-1}). The Stoke's ionic radius r_i for each ion was then estimated by solving Eq. 6 for r_i:

$$u_i = |z_i|\, e/6\pi r_i \eta \tag{6}$$

where e is the electronic charge, and η is the viscosity of the solution. Ionic diffusivities at infinite dilution were also calculated from the ionic mobilities according to

$$D_i = u_i \frac{kT}{|z_i|\, e} = u_i \frac{RT}{|z_i| F} \tag{7}$$

Equation 7 reduces to the relationship generally used for diffusion, $D = u_{abs} kT$ because $\frac{u_{conv}}{|z_i|e} = u_{abs}$. Equation 7 is also a modified form of the Nernst–Einstein equation.[38]

Salt diffusivities were calculated according to the Nernst–Hartley relationship[44] based on limiting equivalent ionic conductances (Eq. 8a),

$$D_{salt} = \frac{(v_+ + v_-)\, \lambda_+^0 \lambda_-^0}{v_+ |z_+| \left(\lambda_+^0 + \lambda_-^0\right)} \frac{RT}{F^2} \tag{8a}$$

which is equivalent to other more commonly reported salt diffusivity relationships.[37,44,47] Electroneutrality (i.e., $\nu_1 z_1 + \nu_2 z_2 = 0$) allows for an equivalent expression of Eq. 8a in terms of valences and transport numbers:

$$D_{salt} = \frac{(|z_+| + |z_-|)\, t_+ t_- \Lambda^0}{|z_+ z_-|} \frac{RT}{F^2} \tag{8b}$$

Equations 5, 7, 8a, and the electroneutrality relationship can be combined to yield equivalent conductance in terms of salt and ionic diffusivities according to Eq. 9,

$$\Lambda^0_{salt} = \frac{(|z_+| + |z_-|)\, D_+ D_-}{D_{salt}} \frac{F^2}{RT} \tag{9}$$

An attempt was made to relate the values of ${\Lambda^0}_{skin}$ and ${\Lambda^0}_{soln}$ to parameters related to the skin's porous pathway as defined by other investigators.[7,9,29–32] In general terms, the permeability of this pathway is usually defined as[29]

$$P_{skin} = \frac{\varepsilon D_{aq} H(\lambda_p)}{\tau L} \tag{10}$$

where ε is porosity, D_{aq} is aqueous diffusivity of the permeant, $H(\lambda_p)$ is the hindrance factor, τ is tortuosity, and L is the membrane thickness. In Eq. 10, λ_p is the ratio of the permeant radius to that of the pore, $\lambda_p = r_s / r_p$, and should not be confused with ionic conductance. We show in Appendix 1 that the following relationship holds for each electrolyte:

$$\frac{\Lambda^0_{skin}}{\Lambda^0_{soln}} = \frac{\varepsilon H(\lambda) h}{\tau L} \frac{(t_+ t_-)_{soln}}{(t_+ t_-)_{skin}} \tag{11}$$

where h is the corresponding electrode separation distance during skin conductivity measurements and $t_\pm$ are the transport numbers. In calculating the conductance ratio in Eq. 11, ${\Lambda^0}_{soln}$ values measured at 25°C were multiplied by 1.15 to correct them to 32°C; this corresponds to an increase in electrolyte conductance of approximately 2% for every 1°C rise in temperature.[48,49] For our calculations, we used h = 4.07 cm and a hydrated SC membrane thickness L = 0.0043 cm (43 μm)[50] to allow an estimate of ε/τ to be derived from the molar conductance ratio and Eq. 11. As the permeants were small with respect to the estimated pore size, we used the Renkin model for hindrance of a spherical permeant diffusing through a cylindrical pore as recommended by Deen.[51] The value of H (λ_p), based on the larger of the two ionic radii was thus given by

$$H(\lambda_p) = (1 - \lambda_p)^2 (1 - 2.104\lambda_p + 2.09\lambda_p^3 - 0.95\lambda_p^5)$$
$$0 < \lambda_p \le 0.4 \tag{12}$$

The pore radius was taken to be 32.5 Å in accord with previous estimates.[7–9] This value differed slightly from the 28 Å value used by Tang et al.[30] to calculate their ε/τ values. We furthermore employed the tortuosity model of Tezel and Mitragotri[8] to estimate τ for each electrolyte. Finally, porosity ε was calculated as the product of τ and ε/τ. Details of this analysis are given in Appendix 2.

Statistical Analysis

One-way analysis of variance (ANOVA) was performed on the NaCl molar conductances at infinite dilution ${\Lambda^0}_{skin}$ measured in each of the experiments,

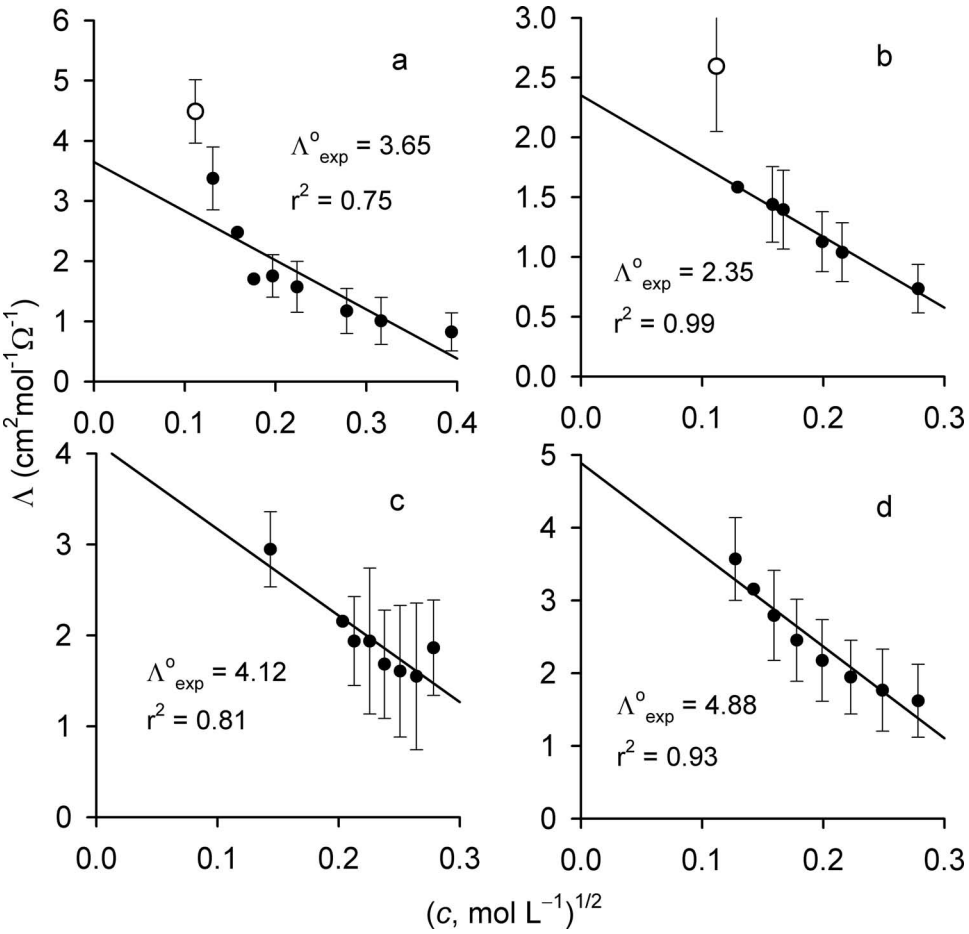

Figure 1. Molar conductance at 32°C of split-thickness human skin immersed in aqueous electrolyte solutions comprised of (a) NaCl, (b) $NiCl_2$, (c) $CrCl_3$, and (d) $K_2Cr_2O_7$. The solid lines show linear regressions of the data according to Eq. 1.

with skin donor as the blocking variable. A p value of less than 0.05 was considered to be significant. A t-test was conducted to assess whether the experimental values of Λ^0_{soln} were significantly different from literature values. A difference corresponding to $p < 0.05$ was considered to be significant.

RESULTS

Representative Kohlrausch plots for electrolytes in skin are shown in Figure 1; the corresponding plots for solutions are provided in the Supplementary Material associated with this manuscript. Skin and solution equivalent conductances at infinite dilution (Λ^0_{skin}, Λ^0_{soln}) obtained from these data are shown in Table 1. These are molar conductances expressed on a charge equivalent basis per standard notation in the literature.[38,43] To relate these values to the molar conductances shown in Figure 1, it should be recognized that Λ^0 ($NiCl_2$) = $2\Lambda^0$ ($\frac{1}{2}NiCl_2$). Solution conductances were in agreement with the literature values to within a maximum error of 16%, with an RMS deviation of 10%. The largest deviations were for the two dichromate salts (+16% for both), followed by $NiSO_4$ (−15%). Agreement for the monovalent electrolytes, NaCl and KCl, was within 1%. The RMS variation of the Λ^0_{soln} determinations, calculated over all electrolytes, was 9%.

Also shown in Table 1 are $\Lambda^0_{skin}/\Lambda_{soln}{}^0$ ratios. The most notable feature is that skin conductances were about 1%–3% of the solution values; equivalently, skin resistance when immersed in a specific electrolyte was higher than that of the electrolyte solution alone by a factor ranging from 36 to 114. $NiCl_2$ and $CrCl_3$ yielded the lowest ratios of $\Lambda^0_{skin}/\Lambda_{soln}{}^0$ at 0.88% each. These ratios reflect the low value of porosity ε for the skin's polar pathway, as well as possible other factors including steric hindrance $H(\lambda_p)$ and tortuosity τ (cf. Eqs. 10 and 11). The Λ^0_{skin} values and any derived associated quantities must, therefore, be considered to be effective properties of the membrane, not absolute values of electrolyte properties within the pores.

Table 1. Limiting Equivalent Conductances of Selected Electrolytes in Aqueous Solution and Skin, Determined as Described in the Text

Salt	Λ^0_{soln} (cm^2 mol^{-1} Ω^{-1})[a] Obs Lit		Λ^0_{skin} (cm^2 mol^{-1} Ω^{-1})[b]	$\Lambda^0_{skin}/\Lambda_{soln}{}^0 \times 100$[c]	References[d]
NaCl	127 ± 8(38)	126.0	4.06 ± 1.59(45)	2.78	38
1/2$NiCl_2$	120 ± 12(10)	123.3	1.22 ± 0.08(15)	0.88	55
1/3 $CrCl_3$	141 ± 5(15)	143.3	1.43 ± 0.45(15)	0.88	49,54
1/2$NiSO_4$	100[e] ± 6(15)	117.5	2.01 ± 0.40(14)	1.74	52
1/2$Ni(NO_3)_2$	121 ± 9(5)	121	1.88 ± 0.35(15)	1.35	49
1/2Na_2CrO_4	134 ± 6(5)	135.2	2.12 ± 0.35 (14)	1.37	49
1/2$Na_2Cr_2O_7$	132 ± 30(5)	113.8	2.22 ± 0.40(14)	1.46	49
1/2K_2CrO_4	158 ± 2(15)	145.1	2.35 ± 0.22(14)	1.30	49,53
1/2$K_2Cr_2O_7$	158[f] ± 6 (15)	136.8	2.59 ± 0.44(15)	1.43	49
KCl	150 ± 12(15)	150	2.12 ± 0.39(15)	1.23	38

[a] 25°C; values expressed as mean ± SD [number of determinations].
[b] 32°C; values expressed as in Footnote (*a*).
[c] Λ^0_{soln} values corrected to 32°C as described in the text.
[d] Reference for literature value of Λ^0_{soln}.
[e] $p < 0.05$.
[f] $p = 0.0085$.

The average skin conductance value for NaCl (mean ± SD, $n = 45$) was 4.06 ± 1.59 cm^2 mol^{-1} Ω^{-1}, reflecting considerable variability between skin samples. ANOVA analysis of these conductances, with donor as the blocking variable, showed no significant difference between the various skin donors ($p = 0.18$). This analysis also revealed that the variance between conductance determinations within skin donors exceeded that between skin donors. This is not usually the case for passive diffusion measurements in skin and may be related to the Franz cell electrode configuration and resulting asymmetrical electric field (making electrode positioning critical). Whatever the reason, no adjustment for donor was made in further analysis of these data. The RMS variation of the Λ^0_{skin} measurements, calculated over all electrolytes, was 23%. A comparison with the 9% variation observed for Λ^0_{soln} determinations highlights the intersample variability of skin tissue.

Cation transport numbers in skin for the four chloride salts, plotted versus average electrolyte concentration C_M, are shown in Figure 2. Limiting transport numbers, calculated by regression of these data versus C_M, are shown in Table 2. Various investigators have extrapolated t^0_+ on either a $\sqrt{c}$ [38] or c [42,45] basis; because the plots in Figure 2 were linear and t_+ values were nearly constant, we chose c as our basis. However, similar calculations based on $\sqrt{c}$ revealed no statistical difference in the results of the ionic conductivity analyses. Corresponding plots for the solution EMF measurements may be found in the Supplementary Material.

Limiting ionic conductances, λ_{soln} and λ_{skin}, obtained from the data in Tables 1 and 2 by the minimization procedure described earlier are shown in Table 3. The uncertainties in these values were based on F-tests at 95% (solution) and 67% (skin) confidence levels, as described in the Methods. The uncertainties in the skin ionic conductance values were much greater than those for the solutions, a finding that results directly from the intersample variability in the skin tissue.

Limiting ionic conductivity values were then used in conjunction with Eqs. 5–7 to calculate ion mobilities, hydrated radii, and effective ionic diffusivities (Table 3). Finally, in conjunction with the relevant Λ^0 value and Eq. 4, they were used to calculate ion transport numbers for all electrolytes in solution and skin (Table 2, columns 4 and 5). The transport numbers for Na^+ and K^+ in chloride solutions are in accord with those available in the literature.[2,4,42] Cation transport number ratios for skin relative to solution were greater than one for Na^+ and K^+, indicating cation permselectivity. However, for the metal salts containing polyvalent cations, these ratios were less than one, demonstrating anion permselectivity. Possible mechanisms for this effect are discussed later.

Time-course resistance experiments were conducted to verify that the level of skin hydration employed in our approach was not adversely affecting the conductance results by compromising skin integrity; details of these investigations are fully discussed in the Supplementary Material. Skin resistance values obtained from these *in vitro* experiments were comparable to literature *in vivo* data.[57,58]

Salt diffusivities at infinite dilution (skin and solution) calculated from ionic diffusivities by means of Eq. 8a are summarized in Table 4. Selected literature values are included for comparison.

Hindrance values $H(\lambda)$, based on the chosen effective radius r_s to be the literature value of the larger ion, were calculated according to Eq. 12. Using these calculated hindrance values, as well as the calculated transport numbers from Table 2 (column 5), porosity/tortuosity estimates for each metal salt were

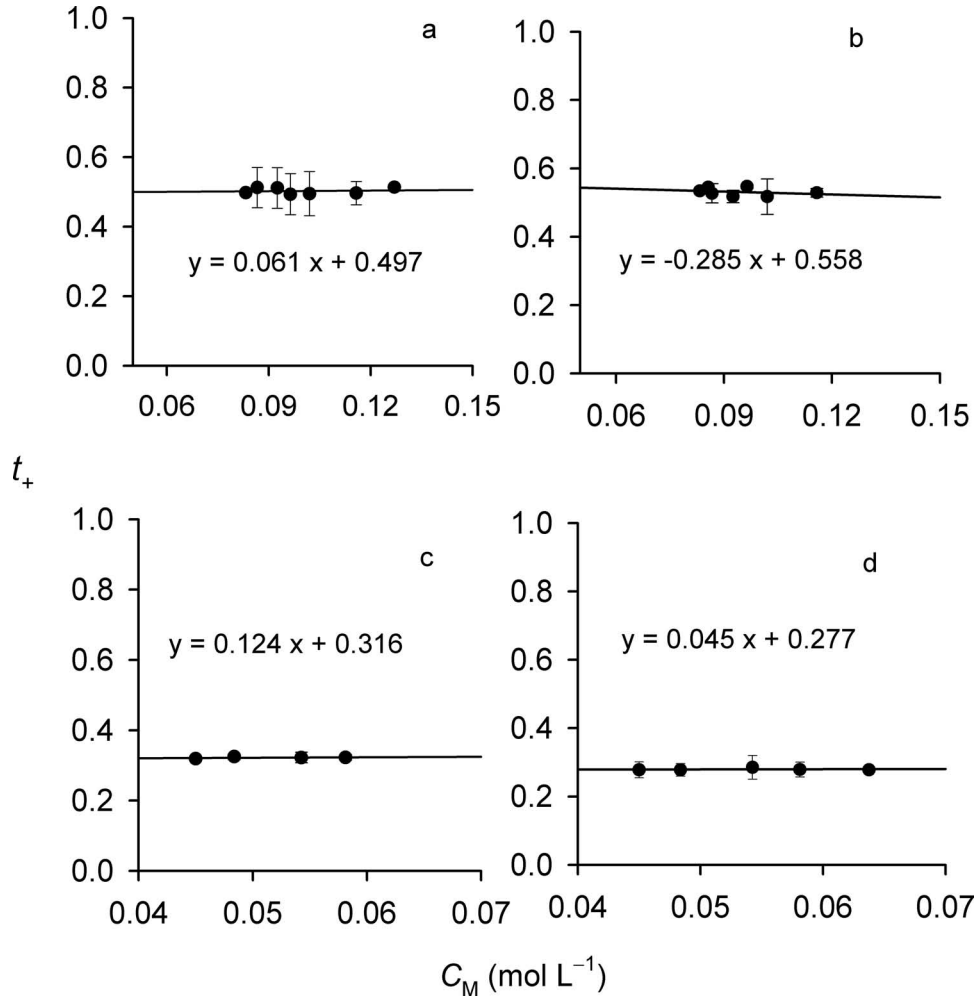

Figure 2. Cation transport number in skin as a function of average (donor and receptor) concentration, C_M, for electrolytes (a) NaCl, (b) KCl, (c) $NiCl_2$, and (d) $CrCl_3$. The solid lines show linear regression of the data to yield extrapolated $t^0{}_+$ values.

calculated according to Eq. 11. Table 5 summarizes these results. Also shown are tortuosity estimates (τ) based on the model of Tezel and Mitragotri[8] (Eq. B.1, Appendix 2) and porosities (ε) calculated as the product of ε /τ and τ. The mean porosity value, $\varepsilon = (1.43 \pm 0.61) \times 10^{-4}$, is within an order of magnitude of most other estimates of this parameter.[7,8,30,31,35] Furthermore, salts tested on the same donors yielded similar values of ε. This is expected because ε is a property of the membrane only.[7,9,35]

Table 2. Cationic Transport Numbers ($t^0{}_+$) Measured in EMF Experiments and Those Calculated from the Ionic Conductivity Values in Table 3 According to Eq. 4

Salt	Solution EMF[a]	Skin EMF[a]	Solution (Eq. 4)	Skin (Eq. 4)	$t_+{}^{skin}/t_+{}^{soln}$ [b]
NaCl	0.41 ± 0.04(9)	0.50 ± 0.07(9)	0.40	0.53	1.33
$NiCl_2$	0.37 ± 0.04(9)	0.32 ± 0.03(9)	0.37	0.31	0.84
$CrCl_3$	0.46 ± 0.05(9)	0.28 ± 0.03(9)	0.46	0.27	0.59
$NiSO_4$	–	–	0.45	0.25	0.56
$Ni(NO_3)_2$	–	–	0.37	0.27	0.73
Na_2CrO_4	–	–	0.38	0.58	1.53
$Na_2Cr_2O_7$	–	–	0.38	0.54	1.42
K_2CrO_4	–	–	0.47	0.61	1.30
$K_2Cr_2O_7$	–	–	0.48	0.57	1.19
KCl	0.50 ± 0.05 (3)	0.56 ± 0.11(3)	0.50	0.56	1.12

[a] Mean ± SD (no. of determinations).
[b] Ratio of column 5 to column 4.

Table 3. Limiting Ionic Conductances (λ), Mobilities (u), and Effective Diffusivities (D) Calculated from the Data in Tables 1 and 2 as Described in the Text

	λ_i (cm^2 mol^{-1} Ω^{-1})		$u \times 10^5$ (cm^2 V^{-1} s^{-1})		$D \times 10^7$ (cm^2 s^{-1})		r_{soln} (Å)	
Salt	Solution[a]	Skin[b]	Solution[a]	Skin[b]	Solution[a]	Skin[b]	Observed	Literature[c]
K^+	75.1 ± 2.8	1.42 ± 0.56	77.9	1.47	200.2	3.87	1.21	1.5
Na^+	51.1 ± 2.5	1.26 ± 0.53	53.0	1.30	136.3	3.42	1.78	2.25
Ni^{2+}	89.9 ± 4.3	1.00 ± 0.47	46.6	0.52	59.9	0.68	4.05	3.0
Cr^{3+}	193.8 ± 6.2	1.21 ± 0.62	66.9	0.42	57.4	0.37	4.23	4.5
Cl^-	75.9 ± 1.6	1.11 ± 0.25	78.7	1.15	202.3	3.01	1.20	1.5
NO_3^-	76.1 ± 2.0	1.38 ± 0.71	78.8	1.43	202.7	3.76	1.20	1.5
SO_4^{2-}	110.1 ± 8.2	3.01 ± 1.39	57.1	1.56	73.4	2.05	3.31	2.0
CrO_4^{2-}	166.2 ± 6.8	1.79 ± 1.36	86.1	0.93	110.8	1.22	2.19	2.0
$Cr_2O_7^{2-}$	163.7 ± 6.8	2.13 ± 1.35	84.9	1.10	109.1	1.45	2.22	2.5[d]

[a] 25°C; values given as mean ± uncertainty at 95% confidence level.
[b] 32°C; values given as mean ± uncertainty at 67% confidence level.
[c] Values taken from Ref. 56.
[d] Estimated value.

Table 4. Salt Diffusivities at Infinite Dilution in Solution and Skin Calculated According to the Nernst–Hartley Relationship, Eq. 8a

	$D_{salt} \times 10^7$ (cm^2 s^{-1})		
	Solution		Skin
	Equation 8a	Literature	Equation 8a
NaCl	163		3.20
$NiCl_2$	113	115 (Ref. 55)	1.41
$CrCl_3$	124	122 (Ref. 54)	1.07
$NiSO_4$	066		1.02
$Ni(NO_3)_2$	113		1.50
Na_2CrO_4	126		2.14
$Na_2Cr_2O_7$	127		2.35
K_2CrO_4	158	145 (Ref. 53)	2.24
$K_2Cr_2O_7$	155		2.48
KCl	202		3.39

DISCUSSION

The question of the existence of an aqueous-continuous permeation pathway through the SC has engendered much discussion. Such a pathway has been postulated to explain the permeation of highly hydrophilic species such as sugars and inorganic ions—substances to which SC lipids are essentially impermeable.[50] The weaker temperature dependence of SC permeability to these species as compared with lipophilic compounds provides one of the strongest arguments in support of this statement.[59,60] Further support comes from the fact that the specific resistance of human skin even when measured *in vivo* (590–1170 kΩ cm^2) after a 5 min equilibration in normal saline[58] is less than that of a single phospholipid bilayer (~1 MΩ cm^2).[61,62] It has been argued that the polar pathway is mainly an artifact of the damage incurred when skin properties are manipulated electrically or acoustically.[63,64] But the fact that individuals experience skin sensitization to metal allergens—even with mild but recurring exposures such as to the back of a watch[65]—argues that it plays an important role in dermal exposure. In the case of compromised skin, such as the hands of nurses, hairdressers, and cement workers, the polar pathway becomes quite significant. We note that Tregear,[66] many years ago, reported passive permeation of sodium and bromide ions *in vivo* in humans. The polar pathway is thought by many to be comprising a combination of shunt pathways in skin appendages and defects in SC lipids.[7,9,31,67–70] On the basis of the *in vitro* studies, it is size selective with effective pore radii in the range of 25–35 Å.[7,29,30,34,35]

Table 5. Porosities (ε) and Tortuosities (τ) Associated with Ion Transport Through Hydrated Human Skin *In Vitro*, Calculated as Described in the Text

Salt	$\varepsilon/\tau \times 10^5$	τ	$\varepsilon \times 10^4$
NaCl	4.11	7.32	3.01
$NiCl_2$	1.28	6.67	0.85
$CrCl_3$	1.40	5.61	0.75[a]
$NiSO_4$	2.10	6.67	1.40[a]
$Ni(NO_3)_2$	1.82	6.67	1.21[b]
Na_2CrO_4	2.02	7.32	1.47[b]
$Na_2Cr_2O_7$	2.19	7.09	1.26
K_2CrO_4	1.71	7.56	1.28[b]
$K_2Cr_2O_7$	2.01	7.09	1.42[b]
KCl	1.56	8.08	1.55
		Mean ± SD	1.43 ± 0.61

[a] Salts tested on skin donors 3,4,5.
[b] Salts tested on skin donors 4,5,6.

To address the relationship of the present measurements to permeability of human skin *in vivo*, we conducted the normal saline skin conductivity experiments summarized in the Supplementary Material. The average tissue resistance after a 48-h immersion in buffered saline was greater than 100 kΩ cm^2. On the basis of the comparison of these results with other published values of skin resistance,[2,4,58,71] we consider that the *in vitro* model is a reasonable representation of human skin *in vivo*, even after immersion for up to 2 days.

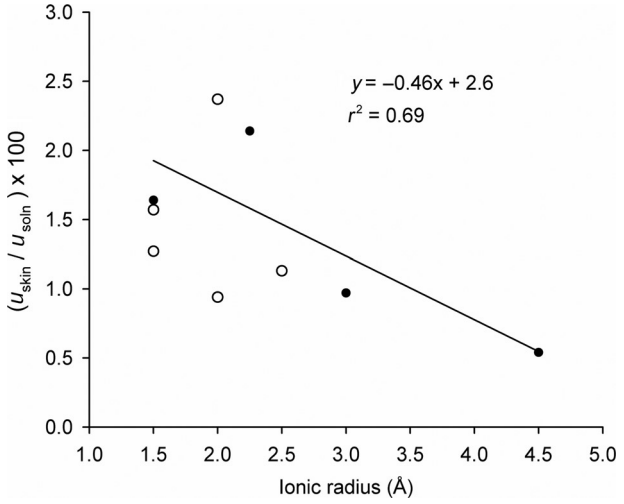

Figure 3. Skin mobility relative to solution as a function of ionic radius of cations (•) and anions (○); solid line corresponds to cationic regression. Restriction resulting from size is clearer for cations than anions because of the greater variation in ionic radii.

Quantitative modeling of the skin's polar pathway has largely been based on the permeation of uncharged, hydrophilic permeants under passive,[29] iontophoretic,[72–74] or sonophoretic[9,30,32,34–36] conditions. Although a few ions like sodium,[2,4,57,58] chloride,[58] and tetraethyl ammonium[75] have received attention, wide variation exists in literature permeation data for metal allergens.[6,10–24] Development of a predictive skin absorption model requires either accurate permeation data or diffusivities for the permeants of interest, in addition to other parameters unique to the polar pathway—porosity, hindrance factor, and tortuosity.

According to Cussler,[37] conductance measurements offer a facile approach for characterizing the diffusion of strong electrolytes such as metal salts through membranes. For potential measurements to be indicative of passive diffusion ion permeability, one must assume that the ions permeate entirely through the membrane, without any endogenous membrane ions contributing to the total ion permeation. In this study, we investigated the conductivity of hydrated skin immersed in electrolyte solutions and found an inverse linear correlation between molar conductance values and the square root of concentration, similar to the Kohlrausch behavior displayed in solutions alone (cf. Fig. 1). Skin equivalent conductances at infinite dilution, Λ^0_{skin}, were of primary interest as a conservative estimator for risk assessment. We found a 36–114-fold reduction in skin molar conductances compared with those in solution, which could be interpreted on the basis of microporous membrane properties (Eq. 11). In Table 1, these values are reported on a charge equivalent basis to provide a clearer picture of the restrictions imposed by membrane diffusion. The fact that the ratio $\Lambda^0_{skin}/\Lambda 0soln$ is substantially lower for salts of divalent and trivalent ions as compared with NaCl is evidence of such restrictions (Table 1). For cations, there is evidence that hydrated ionic radius may play an important role in this selectivity. This may be seen from Figure 3, which shows that the ratio of ionic mobility in skin to that in solution falls off with increasing hydrated radius. The trend for anions is less compelling; however, the size range of the tested species was small.

In regards to the oft-repeated statement that the skin is permselective for cations,[1–4] Table 2 shows that this is not always the case. It is permselective for the monovalent cations Na^+ and K^+. However, just the opposite effect was found for the polyvalent ions Ni^{2+} and Cr^{3+}, at least with the counterions tested; this is in accord with the literature.[3] The degree of cation permselectivity is quantified by the skin/solution transport number ratios shown in Table 2. The reduced transport numbers for polyvalent cations may in part be related to pH, as the solutions were intentionally left unbuffered. For example, Gammelgaard et al.[17] reported pH values of 4.2 and 2.9 for 0.5% potassium dichromate and 0.034 M $CrCl_3$ solutions, respectively. Let us assume similar pH values prevailed in the present conductivity experiments. As the isoelectric point of skin is approximately 4.0 (range 3–4.6),[2,76–79] the skin would be positively charged in $CrCl_3$ solutions and close to neutral in $K_2Cr_2O_7$ solutions. These conditions would favor the permeation of Cl^- versus Cr^{3+}, but would not explain the cation permselectivity for $K_2Cr_2O_7$. Thus, the hydrated size of the polyvalent cations (Fig. 3) is a more likely factor contributing to their poor permeation. Furthermore, both Ni^{2+} and Cr^{3+} have been shown to bind to skin proteins; Ni^{2+} does so reversibly,[12,80] whereas Cr^{3+} binding is stable.[11] Such binding may well play a secondary role in the low diffusivities of these two species in skin (Table 3) and associated cation transference numbers (Table 2).

The salt diffusivity estimates in skin (Table 4, column 4) suggest a mechanism for the higher allergenic potency of $NiCl_2$ ($D_{salt} = 1.41 \times 10^{-7}$ cm^2 s^{-1}) versus $NiSO_4$ ($D_{salt} = 1.02 \times 10^{-7}$ cm^2 s^{-1}).[26] These findings support the Fullerton et al.[16] data on the comparative effect of counterion on nickel salt permeation. They also align with the Gammelgaard et al.[17] finding that oxyanions of Cr^{6+} are better skin permeants than Cr^{3+}, a key result in understanding the allergenic properties of chromium.[27] Confirmation of these predictions with controlled ion permeation measurements is warranted.

DOI 10.1002/jps

CONCLUSIONS

Conductivity measurements for 10 electrolyte solutions, in combination with EMF transport measurements for the four chloride salts in the absence and presence of skin, were used to obtain skin and solution ionic mobilities, diffusivities, and transport numbers. Transport numbers show a permselectivity for monovalent cations (i.e., Na^+ and K^+) in the skin and an inverse dependence on hydrated radius for cation mobilities, reflecting hindrance restrictions in the skin for Ni^{2+} and Cr^{3+} compounds. Effective ionic diffusivities in skin were significantly reduced (~36–114-fold) versus solution values. When interpreted on the basis of existing polar pathway theory, these results were consistent with a tortuosity factor of 5–7 and a membrane porosity of $(1–2) \times 10^{-4}$ for ion permeation through hydrated *stratum corneum*.

Effective diffusivities for the salts in skin calculated from the ionic diffusivity values reported here may aid in predictive skin permeation modeling for metal allergens. Moreover, it seems likely that these results can be extended to the organic ions of interest to industrial concerns and regulatory bodies through additional experimentation and modeling. The rationale for such research is to improve the risk assessment process for highly polar constituents of topical formulations.

ACKNOWLEDGMENTS

This work was supported by grant R01 OH007529 from the National Institute of Occupational Safety and Health (NIOSH). The opinions expressed herein are those of the authors and have not been endorsed by NIOSH. Additional support was provided through an IGERT traineeship for TDL from the National Science Foundation.

Appendix 1

DERIVATION OF Eq. 11

Consider the space between the sensing electrodes in the diffusion cell to consist of two media in series, the aqueous electrolyte solution and the skin. The permeability of the skin in terms of the polar pathway parameters can be defined as

$$P_{\text{skin}} = \frac{\varepsilon D_{\text{aq}} H(\lambda)}{\tau L} \tag{A.1}$$

Likewise, the permeability of the aqueous solution alone can be defined as

$$P_{\text{soln}} = \frac{D_{\text{aq}} K}{h} \tag{A.2}$$

where K, the partition coefficient, equals 1. Thus, a ratio of these two terms yields

$$\frac{P_{\text{skin}}}{P_{\text{soln}}} = \frac{\varepsilon H(\lambda) h}{\tau L} \tag{A.3}$$

However, permeability is also proportional to diffusivity, as calculated by the Nernst–Hartley[44] relationship (Eq. 7b). Expressed in conductance terms for solution only, this would be

$$P_{\text{soln}} \propto D_{\text{soln}} = \frac{RT}{F^2} \frac{|z_+| + |z_-|}{|z_+ z|} \Lambda^0_{\text{soln}} (t_+ t_-)_{\text{soln}} \tag{A.4}$$

and likewise for the polar pathway in skin

$$P_{\text{skin}} \propto D_{\text{skin}} = \frac{RT}{F^2} \frac{|z_+| + |z_-|}{|z_+ z_-|} \Lambda^0_{\text{skin}} (t_+ t_-)_{\text{skin}} \tag{A.5}$$

A ratio of permeabilties in terms of conductivities yields

$$\frac{P_{\text{skin}}}{P_{\text{soln}}} = \frac{\Lambda^0_{\text{skin}}}{\Lambda^0_{\text{slon}}} \frac{(t_+ t_-)_{\text{skin}}}{(t_+ t_-)_{\text{soln}}} \tag{A.6}$$

Hence, combining Eqs. A.3 and A.6 yields:

$$\frac{\Lambda^0_{\text{skin}}}{\Lambda^0_{\text{slon}}} = \frac{\varepsilon H(\lambda) h}{\tau L} \frac{(t_+ t_-)_{\text{soln}}}{(t_+ t_-)_{\text{skin}}} \tag{A.7}$$

which is Eq. 11 in the text.

Appendix 2

TORTUOSITY AS A FUNCTION OF PERMEANT SIZE ONLY

Although a variety of geometrical arrangements for a porous pathway in *stratum corneum* may be envisioned, a cubical lattice of cylindrical pores has been used for the sake of simplicity. Tezel and Mitragotri[8] assumed such a model. This approach yielded an equation for tortuosity based on several permeant and membrane parameters. A least squares fitting of their equation under conditions specific to passive diffusion (see full details in the Supplementary Material) yielded a simpler relationship for passive tortuosity based solely on permeant size, r_s (Å):

$$\tau = 0.2705 \exp\left[88.7418/(r_s + 24.4491)\right] \tag{B.1}$$

REFERENCES

1. Kim A, Green PG, Giriah R, Guy RH. 1993. Convective solvent flow across the skin during iontophoresis. Pharm Res 10:1315–1320.
2. Burnette RR, Ongpipattanakul B. 1987. Characterization of the permselective properties of excised human skin during iontophoresis. J Pharm Sci 76:765–773.

3. Burnette RR, Ongpipattanakul B. 1988. Characterization of the pore transport properties and tissue alteration of excised human skin during iontophoresis. J Pharm Sci 77:132–137.
4. Kasting GB, Bowman LA. 1990. DC electrical properties of frozen, excised human skin. Pharm Res 7:134–143.
5. Cefic. 2012. Request for Proposals: LRI-B13: Development of an in silico model of dermal absorption. Brussels, Belgium: Cefic.
6. Guy RH, Hostynek JJ, Hinz RS, Lorence CR. 1999. Metals and the skin. Topical effects and systemic absorption. New York: Marcel Dekker, Chapters 13 and 25.
7. Mitragotri S. 2003. Modeling skin permeability to hydrophilic and hydrophobic solutes based on four permeation pathways. J Control Release 86:69–92.
8. Tezel A, Mitragotri S. 2003. On the origin of size-dependent tortuosity for permeation of hydrophilic solutes across the stratum corneum. J Control Release 86:183–186.
9. Tezel A, Sens A, Mitragotri S. 2003. Description of transdermal transport of hydrophilic solutes during low-frequency sonophoresis based on a modified porous pathway model. J Pharm Sci 92:381–393.
10. Mali J, Van Kooten W, Van Nerr F. 1963. Some aspects of the behaviour of chromium compounds in the skin. J Invest Dermatol 41:111–122.
11. Samitz M, Katz S, Scheiner D, Gross P. 1969. Chromium-protein interactions. Acta Derm Venereol 49:142–146.
12. Samitz M, Katz S. 1976. Nickel-epidermal interactions: Diffusion and binding. Environ Res 11:34–39.
13. Wahlberg J. 1965. Percutaneous absorption of sodium chromate, cobaltous and mercuric chlorides through excised human and guinea pig skin. Acta Derm Venereol 45:415–426.
14. Lierde V, Chery C, Roche N, Monstrey S, Moens L, Vanhaecke F. 2006. *In vitro* permeation of chromium species through porcine and human skin as determined by capillary electrophoresis-inductively coupled plasma-sector field mass spectrometry. Anal Bioanal Chem 384:378–384.
15. Fullerton A, Andersen J, Hoelgaard A. 1988. Permeation of nickel through human skin *in vitro*—effect of vehicles. Br J Dermatol 118:509–513.
16. Fullerton A, Andersen J, Hoelgaard A, Menne T. 1986. Permeation of nickel salts through human skin *in vitro*. Contact Dermatitis 15:173–177.
17. Gammelgaard B, Fullerton A, Avnstorp C, Menne T. 1992. Permeation of chromium salts through human skin *in vitro*. Contact Dermatitis 27:302–310.
18. Emilson A, Lindberg M, Forslind B. 1993. The temperature effect on *in vitro* penetration of sodium lauryl sulfate and nickel chloride through skin. Acta Derm Venereol 73:203–207.
19. Larese F, Gianpietro A, Venier M, Maina G, Renzi N. 2007. *In vitro* percutaneous absorption of metal compounds. Toxicol Lett 170:49–56.
20. Larese F, D'Aostino F, Crosera M, Adami G, Bovenzi M, Maina G. 2008. *In vitro* percutaneous absorption of chromium powder and the effect of skin cleanser. Toxicol In Vitro 22:1562–1567.
21. Tanojo H, Hostynek J, Mountford H, Maibach H. 2001. *In vitro* permeation of nickel salts through human stratum corneum. Acta Derm Venereol Suppl (Stockh) 212:19–23.
22. Liden S, Lundberg E. 1979. Penetration of chromium in intact human skin *in vivo*. J Invest Dermatol 72:42–45.
23. Hostynek J, Dreher F, Nakada T, Schwindt D, Anigbogu A, Maibach H. 2001. Human stratum corneum absorption by nickel salts. Acta Derm Venereol Suppl (Stockh) 212:11–18.
24. Baranowska-Dutkiawicz B. 1981. Absorption of hexavalent chromium by skin in man. Arch Toxicol 47:47–50.
25. Lagowski J. 1973. Modern inorganic chemistry. New York: Marcel Dekker, pp 669.
26. Hostynek J. 2003. Factors determining percutaneous metal absorption. Food Chem Toxicol 41:327–345.
27. Rom W, Markowitz S. 2007. Environmental and occupational medicine. 4th ed. Philadelphia: Lippincott, Williams, and Wilkins, pp 1053.
28. Bodde HE, van den Brink I, Koerten HK, de Haan FHN. 1991. Visualization of *in vitro* percutaneous penetration of mercuric chloride transport through intercellular space versus cellular uptake through desmosomes. J Control Release 15:227–236.
29. Peck K, Ghanen A, Higuchi W. 1994. Hindered diffusion of polar molecules through and effective pore radius estimates of intact and ethanol treated human epidermal membrane. Pharm Res 11:1306–1314.
30. Tang H, Mitragotri S, Blankschtein D, Langer RS. 2001. Theoretical description of transdermal transport of hydrophilic permeants: Application to low-frequency sonophoresis. J Pharm Sci 90:545–568.
31. Kushner J, Blankschtein D, Langer R. 2007. Evaluation of the porosity, the tortuosity, and the hindrance factor for the transdermal delivery of hydrophilic permeants in the context of the aqueous pore pathway hypothesis using dual-radiolabeled permeability experiments. J Pharm Sci 96:3263–3282.
32. Tezel A, Sens A, Mitragotri S. 2002. Incorporation of lipophilic pathways into the porous pathway model for describing skin permeabilization during low frequency sonophoresis. J Control Release 83:183–188.
33. Tang H, Blankschtein D, Langer R. 2002. Prediction of steady-state skin permeabilities of polar and nonpolar permeants across excised pig skin based on measurements of transient diffusion: Characterization of hydration effects on the skin porous pathway. J Pharm Sci 91:1891–1907.
34. Tang H, Blankschtein D, Langer R. 2002. Effects of low-frequency ultrasound on the transdermal permeation of mannitol: Comparative studies with *in vivo* and *in vitro* skin. J Pharm Sci 91:1776–1794.
35. Tezel A, Sens A, Mitragotri S. 2002. A theoretical analysis of low-frequency sonophoresis: Dependence of transdermal transport pathways on frequency and energy density. Pharm Res 19:1841–1846.
36. Tezel A, Sens A, Tuchscherer J, Mitragotri S. 2002. Synergistic effect of low frequency ultrasound and surfactants on skin permeability. J Pharm Sci 91:91–100.
37. Cussler EL. 1997. Diffusion: Mass transfer in fluid systems. 2nd ed. Cambridge: Cambridge University Press, pp 143–154.
38. Bockris JOM, Reddy AKN. 1970. Modern electrochemistry. Vol. I. New York: Plenum Press, pp 355–84, 400–402.
39. Merritt EW, Cooper ER. 1984. Diffusion apparatus for skin penetration. J Control Release 1:161–162.
40. Amang D, Alexandrova S, Schaetzel P. 2003. The determination of diffusion coefficients of counter ion in an ion exchange membrane using electrical conductivity measurements. Electrochem Acta 48:2563–2569.
41. Davies D, Ward R, Heylings J. 2004. Multi-species assessment of electrical resistance as a skin integrity marker for *in vitro* percutaneous absorption studies. Toxicol In Vitro 18:351–358.
42. Aguilella V, Kontturi K, Murtomaki L, Ramirez P. 1994. Estimation of the pore size and charge density in human cadaver skin. J Control Release 32:249–257.
43. Moore WJ. 1972. Physical chemistry. 4th ed. Englewood Cliffs, New Jersey: Prentice-Hall, pp 425–435.
44. Robinson R, Stokes R. 1965. Electrolyte solutions. 2nd ed. London, UK: Butterworths, pp 284–288.
45. Lakshminarayanaiah N. 1969. Transport phenomena in membranes. New York: Academic Press, pp 69.
46. Bevington PR. 1969. Data reduction and error analysis for the physical sciences. New York: McGraw-Hill, pp 117.
47. Lide DR, Ed. 2004. CRC handbook of physics and chemistry. 85th ed. Boca Raton: CRC Press, pp 1089.

48. Barron J, Ashton C. 2007. The effect of temperature on conductivity measurement. County Clare, Ireland: Reagecon Diagnostics, Ltd.
49. Jones H, Jacobson C. 1908. The conductivity and ionization of electrolytes in aqueous solutions as conditioned by temperature, dilution, and hydrolysis. Am J Chem 40:355–407.
50. Wang T-F, Kasting GB, Nitsche JM. 2007. A multiphase microscopic model for stratum corneum permeability. II. Estimation of physicochemical parameters and application to a large permeability database. J Pharm Sci 96:3024–3051.
51. Deen WM. 1987. Hindered transport of large molecules in liquid-filled pores. AIChE J 33:1409–1425.
52. Tsierkezos N, Molinou I. 2000. Limiting molar conductances and thermodynamic association constants for nickel, cadmium, magnesium, and copper sulfates in mixtures of methanol and water at 293.15 K. J Chem Eng Data 45:819–822.
53. Iadicicco N, Paduano L, Vitagliano V. 1996. Diffusion coefficients for the system potassium chromate–water at 25°C. J Chem Eng Data 41:529–533.
54. Riberio ACF, Lobo VM, Oliveira LRC, Burrows HD, Azevedo EFG, Fangaia SIG, Nicolau PMG, Guerra FADRA. 2005. Diffusion coefficients of chromium chloride solutions in aqueous solutions at 298.15 K and 303.15 K. J Chem Eng Data 50:1014–1017.
55. Stokes R, Phang S, Mills R. 1979. Density, conductance, transference numbers, and diffusion measurements in concentrated solutions of $NiCl_2$ at 25°C. J Soln Chem 8:489–500.
56. Kielland J. 1937. Individual activity coefficients of ions in aqueous solutions. J Am Chem Soc 59:1675–1678.
57. Tregear RT. 1966. Physical functions of skin. New York: Academic Press, pp 53–64.
58. Tregear RT. 1965. Interpretation of skin impedance measurements. Nature 205:600–601.
59. Peck KD, Ghanem A-H, Higuchi WI. 1995. The effect of temperature upon the permeation of polar and ionic solutes through human epidermal membrane. J Pharm Sci 84:975–982.
60. Mitragotri S. 2007. Temperature dependence of skin permeability to hydrophilic and hydrophobic solutes. J Pharm Sci 96:1832–1839.
61. Huang C, Wheeldon L, Thompson T. 1964. The properties of lipid bilayer membranes separating two aqueous phases: Formation of a membrane of simple composition. J Mol Biol 8:148–160.
62. Tsong T. 1991. Electroporation of cell membranes. Biophys J 60:297–306.
63. Cullander C, Guy RH. 1991. Sites of iontophoretic current flow into the skin: Identification and characterization with the vibrating probe electrode. J Invest Dermatol 97:55–64.
64. Weaver JC, Vaughan TE, Chizmadzhev Y. 1999. Theory of electrical creation of aqueous pathways across skin transport barriers. Adv Drug Deliv Rev 35:21–39.
65. Hemingway J, Molokhia M. 1987. The dissolution of metal nickel in artificial sweat. Contact Dermatitis 16:99–105.
66. Tregear RT. 1966. The permeability of mammalian skin to ions. J Invest Dermatol 48:16–23.
67. Potts R, Guy R, Francoeur M. 1992. Routes of ionic permeability through mammalian skin. Solid State Ionics 53:165–169.
68. Wahlberg JE. 1968. Transepidermal or transfollicular absorption? Acta Derm Venereol 48:336–344.
69. Grimnes S. 1984. Pathways of ionic flow through human skin *in vivo*. Acta Derm Venereol 64:93–98.
70. Cullander C. 1992. What are the pathways of iontophoretic current flow through mammalian skin? Adv Drug Deliv Rev 9:119–135.
71. Li SK, Higuchi WI, Zhu H, Kern SE, Miller DJ, Hastings MS. 2003. *In vitro* and *in vivo* comparisons of constant resistance AC iontophoresis and DC iontophoresis. J Control Release 91:327–343.
72. Pikal MJ, Shah S. 1990. Transport mechanisms in iontophoresis. III. An experimental study of the contributions of electroosmotic flow and permeability change in transport of high and low molecular weight solutes. Pharm Res 7:222–229.
73. Peck KJ, Srinivasan V, Li SK, Higuchi WI, Ghanem A-H. 1996. Quantitative description of the effect of molecular size upon electroosmotic flow enhancement during iontophoresis for a synthetic membrane and human epidermal membrane. J Pharm Sci 85:781–788.
74. Sims SM, Higuchi WI, Srinivasan V. 1991. Skin alteration and convective solvent flow effects during iontophoresis. Int J Pharm 69:109–121.
75. Srinivasan V, Sims SM, Higuchi WI, Behl CR, Malick AW, Pons S. 1990. Iontophoretic transport of drugs: A constant voltage approach. In Pulsed and Self-regulated Drug Delivery; Kost J, Ed. Boca Raton, Florida: CRC Press, Chapter 4, pp. 65–92.
76. Lai P, Roberts MS. 1999. An analysis of solute structure-human epidermal transport relationships in epidermal iontophoresis using ionic mobility pore model. J Control Release 58:323–333.
77. Wise DL, Ed. 2000. Handbook of pharmaceutical controlled-release technology. New York: CRC Press, pp 633.
78. Pikal MJ, Shah S. 1990. Transport mechanisms in iontophoresis. II. Electroosmotic flow and transference number measurements for hairless mouse skin. Pharm Res 7:213–221.
79. Rosendal T. 1943. Studies on conductance properties of human skin to direct current. Acta Physiol Scand 5:130–151.
80. Fullerton A, Hoelgaard A. 1988. Binding of nickel to human epidermis *in vitro*. Br J Dermatol 119:675–682.

Human Skin is Permselective for the Small, Monovalent Cations Sodium and Potassium But Not for Nickel and Chromium

Terri D. La Count and Gerald B. Kasting*
Winkle College of Pharmacy

The University of Cincinnati Academic Health Center

Supplementary Material

Equations, tables and figures designated solely by a number (i.e. "Figure 1", "Table 1", "Eq. 1", etc.) refer to those in the main text. New material introduced in the Supplementary Material is differentiated with a preceding "S" (i.e. " Figure S1", "Table S1", "Eq. S1").

Solution Molar Conductance Measurements

Representative solution conductance graphs are shown in Figure S1. These data were used in the data analysis and also served to test the accuracy of the experimental approach through a comparison with literature values. As with the skin data, the molar conductance data (*n*=6) for each solution concentration were first averaged, and then regressed according to the Kohlrausch Law over the relevant concentration range. Extrapolation to infinite dilution yielded the limiting molar conductance values, Λ_{soln}^{o}, reported in Table 1. In most cases we found that the Franz cell experiments yielded values of Λ^{0}_{soln} in agreement with those in the literature, although the slopes of the Kohlrausch plots were not in as good agreement. Since our analysis focuses on Λ^{0}_{soln} we considered these slope differences to be acceptable. The Λ^{0}_{soln} values for $NiSO_4$ and the dichromates differed from the literature values we have reported by 15% and

16%, respectively. We note, however, that the literature values for these compounds varied with the source. Additionally, interconversion of aqueous chromate and dichromate ions at pH values below 6.5[S1] may have led to closer molar conductance values for these compounds than what is found in the literature.

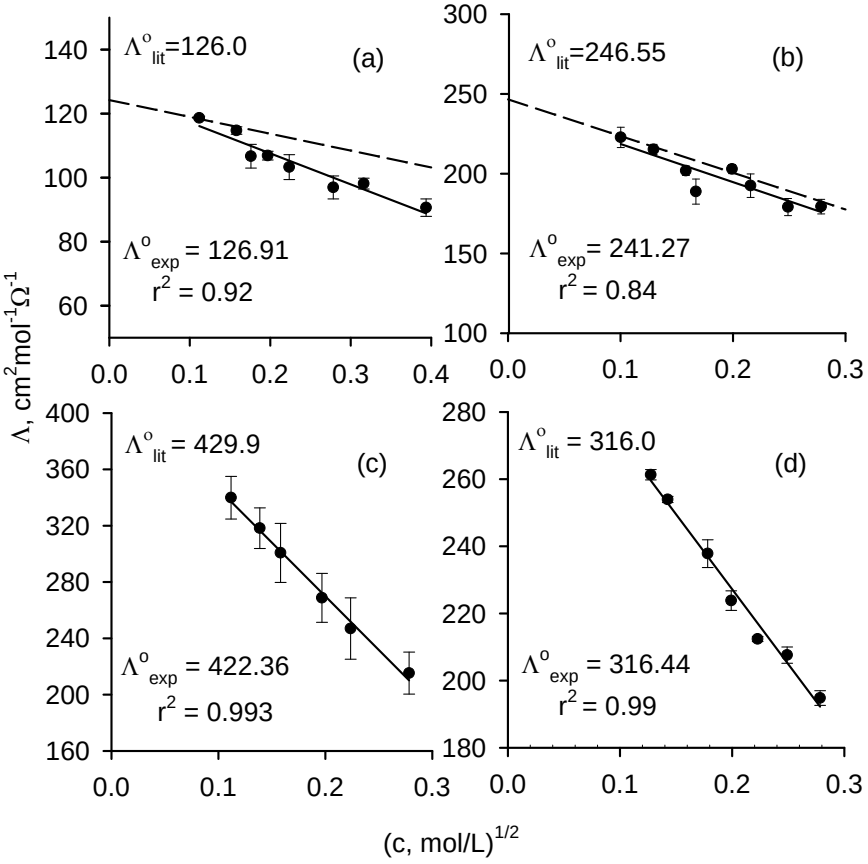

Figure S1. Molar conductance at 25°C of aqueous electrolyte solutions comprised of (a) NaCl; (b) $NiCl_2$; (c) $CrCl_3$; (d) $K_2Cr_2O_7$. The solid lines are linear regressions of the data according to Eq. (1), whereas the dashed lines are linear regressions based on literature data.[S2-S4]

Solution Transport Number Measurements

Figure S2 shows the results of solution cation transport number measurements for the four chloride salts. These transport numbers were plotted as a function of average electrolyte

concentration, C_M, and extrapolated to infinite dilution as shown to obtain t_+^0. A comparison of this approach with t_+^0 values determined by extrapolation on a $\sqrt{c}$ basis yielded no statistical differences. The results of these measurements are summarized in Table 2.

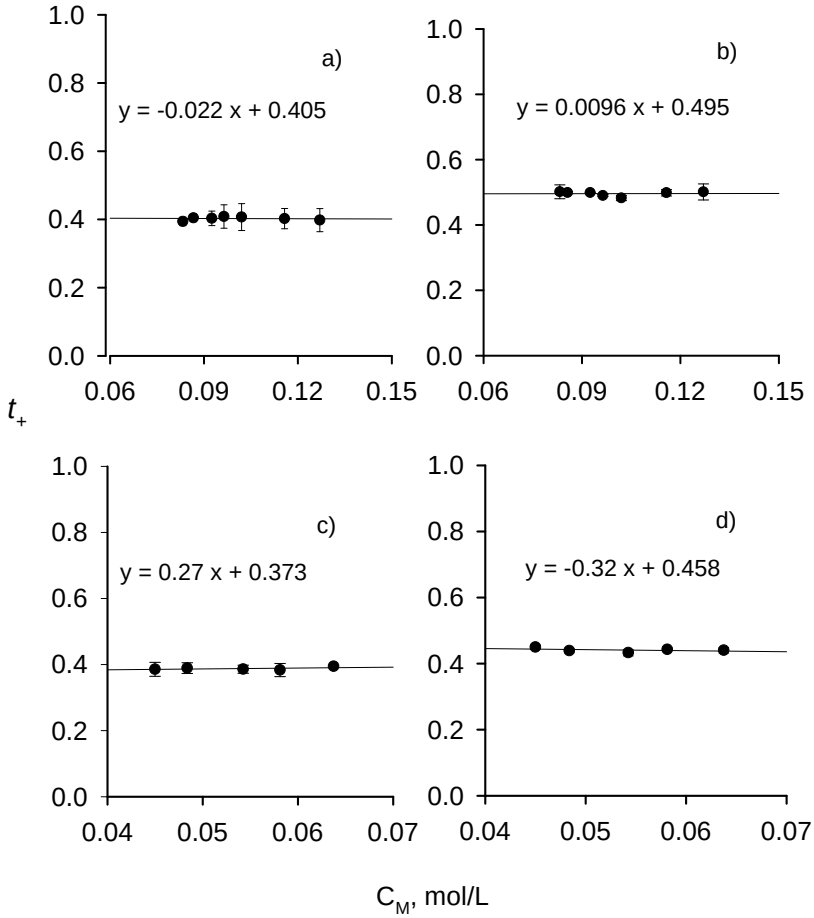

Figure S2. Solution cation transport number as a function of average (donor and receptor) concentration, C_M, for electrolytes (a) NaCl; (b) KCl; (c) $NiCl_2$; (d) $CrCl_3$. The solid lines are linear regressions which yielded extrapolated t_+^0 values at infinite dilution, i.e. zero concentration.

Determination of Error Bounds on $^a\lambda_i$ Values

The limiting values of the ionic conductivities, λ_i, listed in Table 3 were determined by a non linear regression procedure as described in the main text. Uncertainties in these values were determined by varying each value of λ_l around its optimum, re-optimizing the remaining λ_j

values, $j \neq i$, and computing the resulting sum-of-squared residuals, SSR. An *F*-test on the ratio of SSR so computed to that at the optimum yielded the uncertainties. This procedure is shown graphically for select ions in Figures S3 (solution) and S4 (skin).

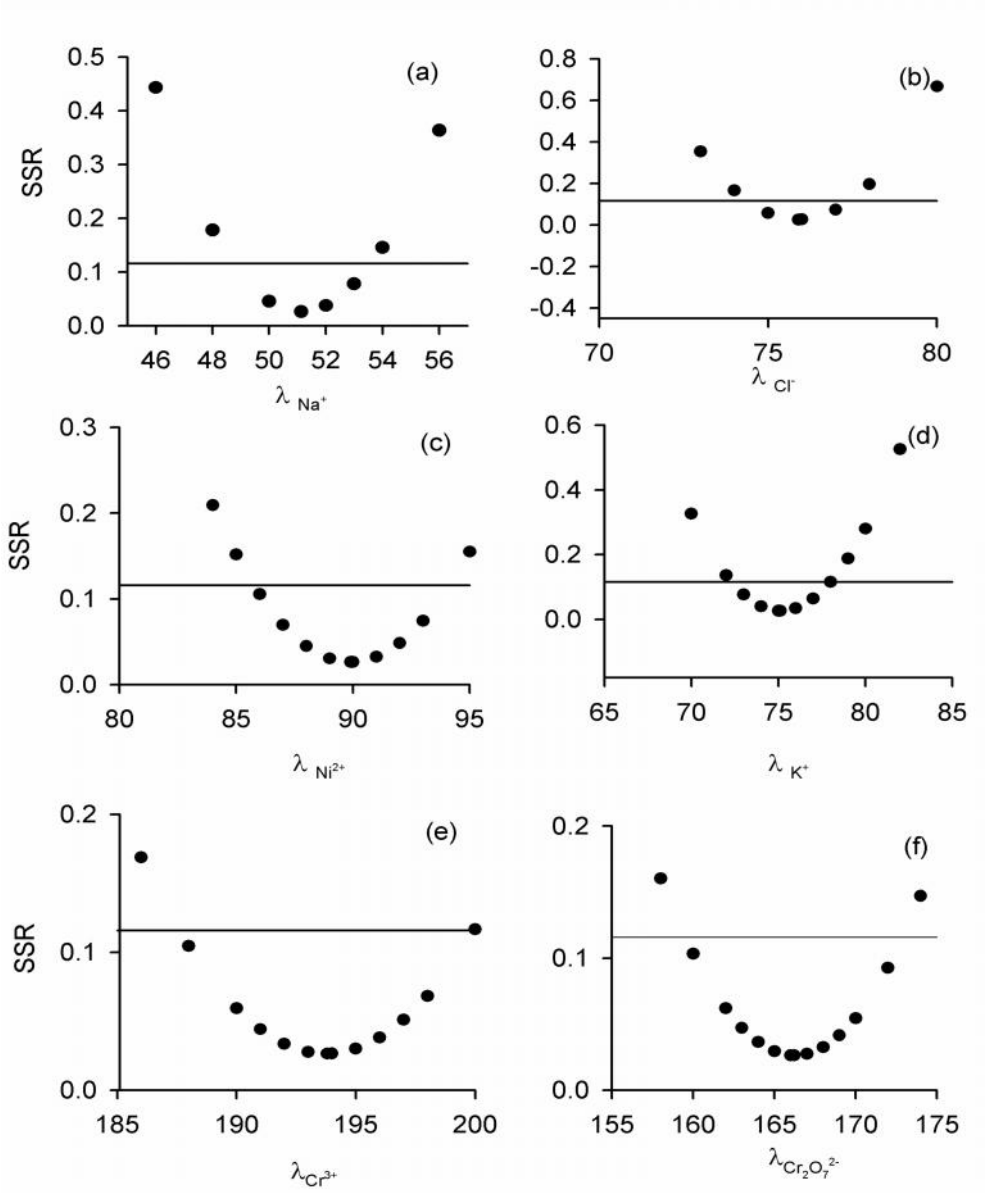

Figure S3. Error plots for ionic conductivities of selected ions in solution. The horizontal solid lines show the value of SSR at the chosen level of significance according to an *F*-test, and the circles show the associated range of λ_j for ions: (a) Na^+; (b) Cl^-; (c) Ni^{2+}; (d) K^+; (e) Cr^{3+}; (f) Cr_2O7^{2-}.

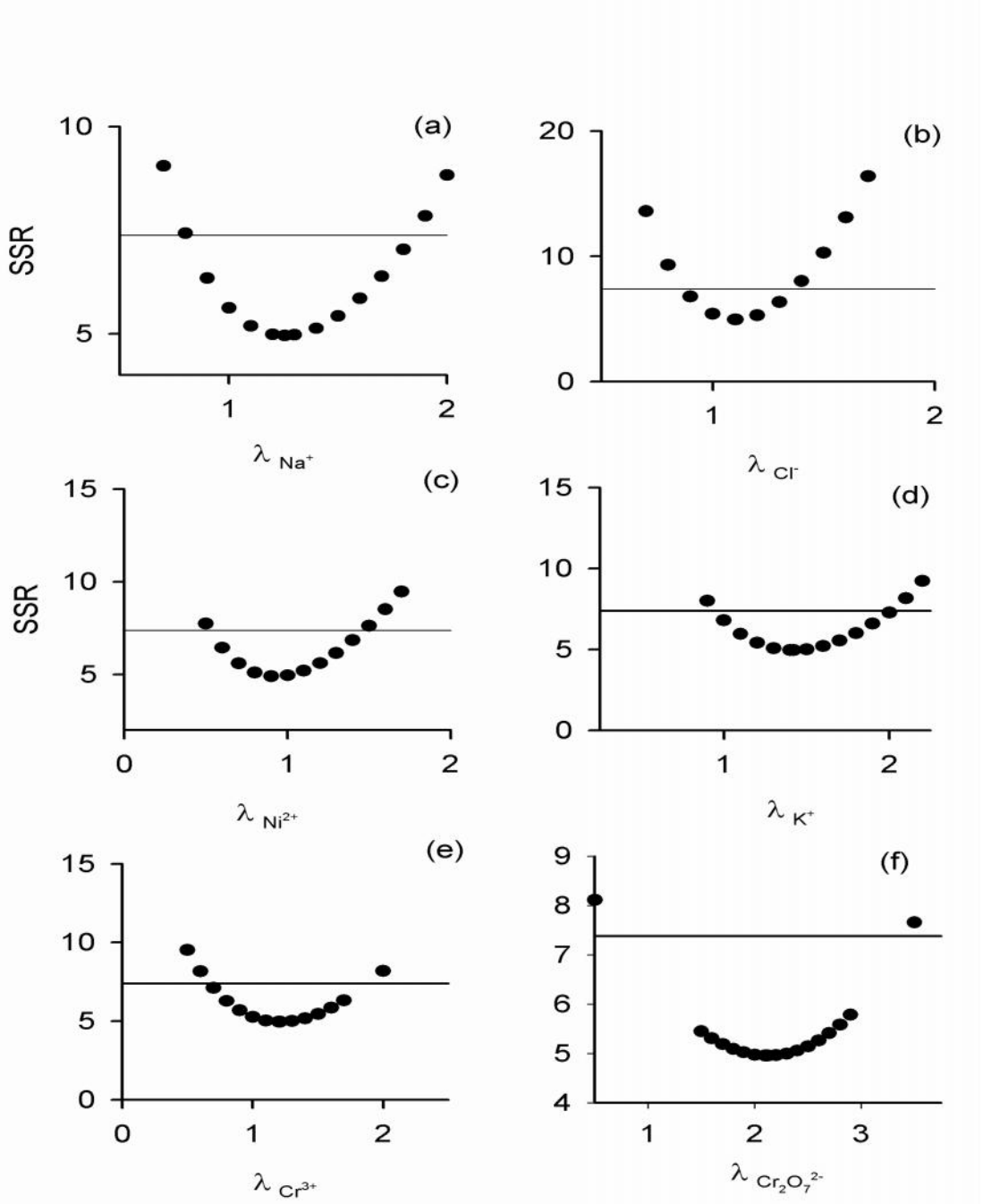

Figure S4. Error plots for ionic conductivities of selected ions in skin. The horizontal solid lines show the value of SSR at the chosen level of significance according to an *F*-test, and the circles show the associated range of λ_j for ions: (a) Na^+; (b) Cl^-; (c) Ni^{2+}; (d) K^+; (e) Cr^{3+}; (f) Cr_2O7^{2-}.

Skin Resistance as a Function of Immersion Time

The time course for split-thickness human skin resistance in Franz diffusion cells with both sides of the tissue bathed in 0.154M NaCl is shown in Figure S5. Skin resistances generally fell to approximately 70% of their initial value during the first 30 minutes of exposure, a period corresponding to rapid hydration of the stratum corneum. This drop was followed by a gradual decline of 10-15 % over the remaining 47.5 h, consistent with the gradual water uptake observed in other *in vitro* experiments.[S5] Similar behavior has been reported elsewhere.[S6-S13] On average, the mean resistivity after 48 h immersion was still 57% of the value measured in the first few seconds of exposure.

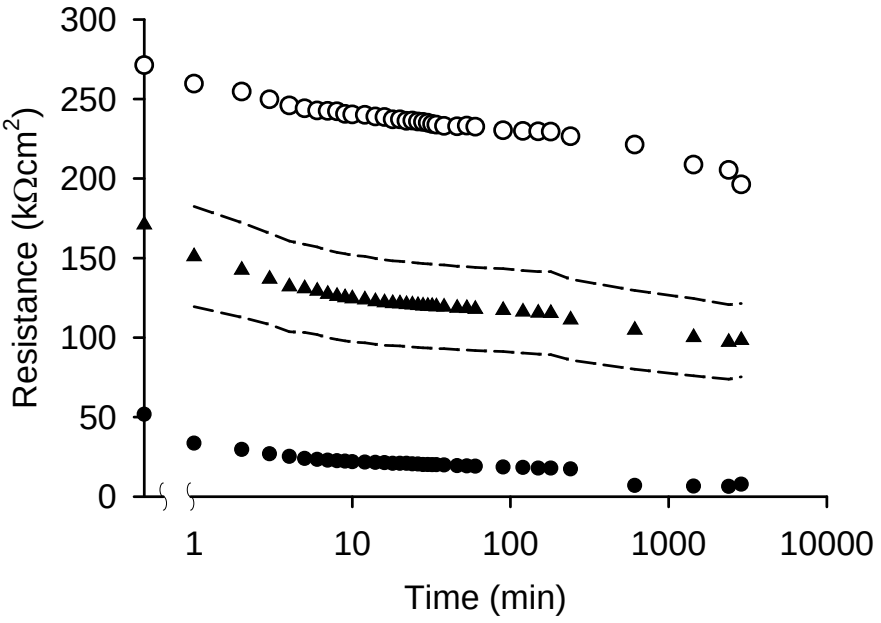

Figure S5. Specific resistance of split-thickness human skin immersed in normal saline solution for 48-hours post-dose. Shown are upper (o) and lower limits (•) for individual samples, and the average of all buffered and buffered solution values (triangles) with 95% CI (dashed lines).

There were no significant differences in resistance between skin samples immersed in buffered and unbuffered solutions (data not shown). The figure shows upper and lower limits of resistance for individual samples (denoted by circles), as well as the average for all measurements and their 95% confidence limits.

The average specific resistance after 5 minutes immersion, 130 $k\Omega cm^2$(20Hz), may be compared with Tregear's range of 590-1170 $k\Omega cm^2$ (1.5 Hz) or 700 $k\Omega cm^2$ (10 Hz) for human dorsal forearm *in vivo.*[S13] Tregear's Figure 1 shows that these values decline to about 400 $k\Omega cm^2$ at 20 Hz due to capacitive effects. If one further allows that the *in vivo* measurements are possibly measuring two skin resistances [S12] and assumes the two surface electrodes were identical, the correspondence becomes even closer. Additional support for the excised skin model is provided by Li et al. [S8], who found that the AC and DC electrical and barrier properties of *in vitro* human epidermal membrane were semi-quantitatively consistent with those of human skin *in vivo*.

Tortuosity of the Polar Pathway as a Function of Permeant Size

This section outlines the development of the tortuosity relationship used to estimate polar pathway tortuosities for the test permeants in Table 5. The physical network most frequently employed in the stratum corneum (SC) polar pathway model[S14-S16] is a cubical lattice arrangement of long cylindrical pores. Using this approach, Tezel et al.[S17] developed a permeant-specific tortuosity model as a function of three key factors: lateral pore separation (δ), pore juncture distance (α), and permeant radius (r_s). Their development took into account a distribution of pore sizes, γ (r_s), whereby a small permeant will experience a greater tortuosity through the SC than a larger one due to the inherently greater number of pores available for

transport. Assumptions included in their analysis are a pore radius of 32.5 Å and skin porosity of 2×10^5.[S17] Assuming a cubical lattice, the latter value yields a δ value of ~1.3 μm.

Tezel et al.[S17] presented a graph of tortuosity as a function of permeant size for two values of α, 1.6 and 3.0, (dashed and dashed/dotted curves in their Figure 5, respectively) and argued that these α values defined a limiting range for possible values of enhanced permeation (i.e. iontophoresis or sonophoresis) for the four polar permeants on which their porosity figure was based. We elected to use a least squares fit of their tortuosity equation

$$^2 = 1 + \frac{4}{5}\left(\frac{¢}{\sim}\right)\sum_{n=1}^{\infty} n \left(\frac{3}{4}\right)^{n-1} \left[\int_{r_p}^{\infty} ¥(r)dr\right]^n \qquad \text{(S1)}$$

to the passive tortuosities displayed, thereby yielding a solid curve (see Figure S6) corresponding to α = 1.85. (Note that in Eq. (S1), their nomenclature for solute radius (r_p) differs from ours (r_s)). Re-parameterization of Eq. (S1) by nonlinear regression into a simpler form yielded a passive tortuosity relationship based solely on permeant size (r_s) which is also given as Eq. (B.1) in Appendix 2:

$$^2 = 0.2705 \exp\left(88.7418/(r_s + 24.4491)\right) \qquad \text{(S2)}$$

Equation (S2) is within graphical accuracy of Eq. (S1), with an rms deviation of 0.025. Hence, further tortuosity calculations were based on Eq. (S2)

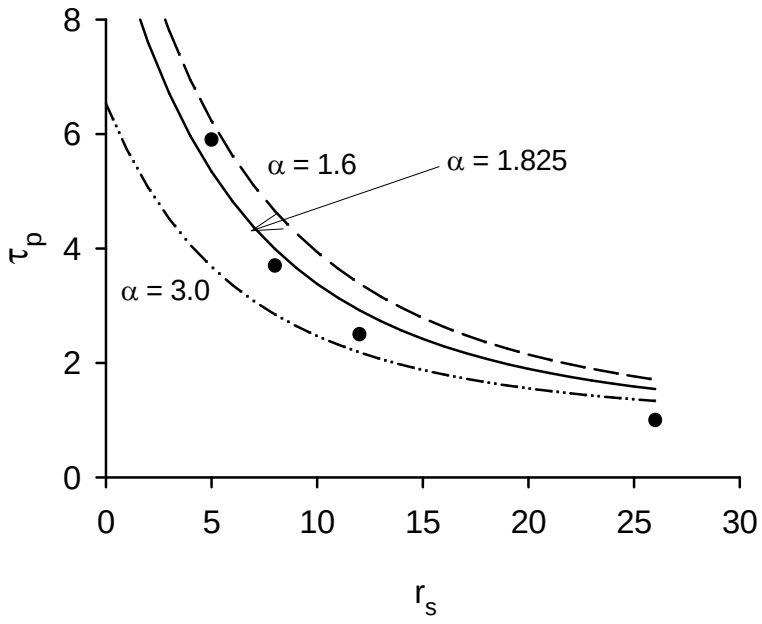

Figure S6. Polar pathway tortuosity as a function of hydrodynamic radius of the permeant according to the model of Tezel et al.[S17] The symbols on the graph represent (left to right) mannitol, LHRH, inulin and dextran. The curves depict the limiting values suggested by Tezel et al. (dashed lines, α = 1.6, 3.0) and a least squares fit to the data (solid line,α = 1.85).

REFERENCES CITED

S1 Raynor-Canham G, Overton T. 2003. Descriptive inorganic chemistry. 3rd ed. New York: WH Freeman. p. 482.

S2 Robinson R, Stokes R. 1965. Electrolyte solutions. 2nd (rev) ed. London: Butterworths. pp.284-88.

S3 Jones H, Jacobson C. 1908. The conductivity and ionization of electrolytes in aqueous solutions as conditioned by temperature, dilution, and hydrolysis. Am J Chem 40:355-407.

S4 Stokes R, Phang S, Mills R. 1979. Density, conductance, transference numbers, and diffusion measurements in concentrated solutions of NiCl2 at 25°C. J Soln Chem 8: 489-500.

S5 Anderson RL, Cassidy JM, Hansen JR, Yellin W. 1973. Hydration of stratum corneum. Biopolymers 12:2789-2802.

S6 Kasting GB, Bowman LA. 1990. DC electrical properties of frozen, excised human skin. Pharm Res 7(2):134-143.

S7 Kasting GB, Bowman LA. 1990. Electrical analysis of fresh, excised human skin: a comparison with frozen skin. Pharm Res 7(11):1141-1146.

S8 Li SK, Higuchi WI, Zhu H, Kern SE, Miller DJ, Hastings MS. 2003. *In vitro* and *in vivo* comparisons of constant resistance AC iontophoresis and DC iontophoresis. J Controlled Rel 91:327-343.

S9 Burnette RR, Bagniefski TM. 1988. Influence of constant current iontophoresis on the impedance and passive Na+ permeability of excised nude mouse skin. J Pharm Sci 77(6):492-497.

S10 Dinh S, Luo C-W, Berner B. 1993. Upper and lower limits of human electrical resistance in iontophoresis. AIChEJ 39:2011-2018.

S11 Rosendal T. 1943. Studies on conductance properties of human skin to direct current. Acta Physiol Scand 5:130-151.

S12 Tregear RT. 1966. Physical functions of skin. New York: Academic Press. pp. 53-64.

S13 Tregear RT. 1965. Interpretation of skin impedance measurements. Nature 205:600-601.

S14 Tang H, Mitragotri S, Blankschtein D, Langer RS. 2001. Theoretical description of transdermal transport of hydrophilic permeants: application to low-frequency sonophoresis. J Pharm Sci 90:545-568.

S15 Tezel A, Sens A, Mitragotri S. 2002. Incorporation of lipophilic pathways into the porous pathway model for describing skin permeabilization during low frequency sonophoresis. J Control Rel 83:183-188.

S16 Tang H, Blankschtein D, Langer R. 2002. Prediction of steady-state skin permeabilities of polar and nonpolar permeants across excised pig skin based on measurements of transient diffusion: characterization of hydration effects on the skin porous pathway. J Pharm Sci 91(8):1891-1907.

S17 Tezel A, Mitragotri S. 2003. On the origin of size-dependent tortuosity for permeation of hydrophilic solutes across the stratum corneum. J Control Rel 86(1):183-186.